Articles

Structural Characterization of a Putative Endogenous Metal Chelator in the Periplasmic Nickel Transporter NikA[†,‡]

Mickaël V. Cherrier,[§,||] Christine Cavazza,[§] Constance Bochot,[§] David Lemaire,[⊥,#] and Juan C. Fontecilla-Camps*[,§]

Laboratoire de Cristallographie et de Cristallogenèse des Protéines, Institut de Biologie Structurale J.P. Ebel, CEA, CNRS, Université J. Fourier, 41 rue J. Horowitz, 38027 Grenoble Cedex 1, France, and Laboratoire de Spectrométrie de Masse des Protéines, Institut de Biologie Structurale J.P. Ebel, CEA, CNRS, Université J. Fourier, 41 rue J. Horowitz, 38027 Grenoble Cedex 1, France

Received June 4, 2008; Revised Manuscript Received August 8, 2008

ABSTRACT: *Escherichia coli* and related bacteria require nickel for the synthesis of hydrogenases, enzymes involved in hydrogen oxidation and proton reduction. Nickel transport to the cytoplasm depends on five proteins, NikA−E. We have previously reported the three-dimensional structure of the soluble periplasmic nickel transporter NikA in a complex with $FeEDTA(H_2O)^-$. We have now determined the structure of EDTA-free NikA and have found that it binds a small organic molecule that contributes three ligands to the coordination of a transition metal ion. Unexpectedly, His416, which was far from the metal-binding site in the $FeEDTA(H_2O)^-$−NikA complex, becomes the fourth observed ligand to the metal. The best match to the omit map electron density is obtained for butane-1,2,4-tricarboxylate (BTC). Our attempts to obtain a BTC−Ni−NikA complex using apo protein and commercial reagents resulted in nickel-free BTC−NikA. Overall, our results suggest that nickel transport in vivo requires a specific metallophore that may be BTC.

INTRODUCTION

Nickel, a rare element generally present at only nanomolar concentrations in the environment (*1*), is nevertheless essential for a variety of microorganisms having enzymes such as NiFe hydrogenases, ureases, acetyl coenzyme A synthases and one class of carbon monooxide dehydrogenases (*1, 2*). In *Escherichia coli* and other related Gram negative bacteria, high affinity Ni transport depends on the *nikA-E* operon. The corresponding proteins, which are only expressed under anaerobic conditions (*3*), belong to the family of ABC-type transporters, generally involved in nutrient and peptide import processes (*4*). The *nik* operon encodes two pore-forming integral inner membrane proteins (NikB and C), two inner membrane-associated proteins with ATPase activity (NikD and E) and a periplasmic Ni-binding protein (NikA). The expression of the Nik proteins is under the direct control of the nickel-binding NikR, a DNA-binding protein whose activity is, in turn, indirectly controlled by the availability of molecular hydrogen (*5, 6*). In *E. coli*, three homologous hydrogenases are Ni-containing enzymes, which activities depend on Ni transport by proteins coded by the *nik* operon.

NikA is a 56 kDa protein of known three-dimensional structure (*7, 8*) that was initially reported to bind a single Ni(II) ion. Heddle et al. (*8*) described the metal binding site of NikA as being a pocket rich in aromatic residues that lodged a $Ni(H_2O)_5^{2+}$ species. However, work from our laboratory has shown that, unexpectedly, aerobically expressed, recombinant NikA binds $Fe(III)EDTA(H_2O)^-$ with high affinity when purified in the presence of the metal chelator (*7*). We have also shown that the same applies to the structure deposited by Heddle et al. who used EDTA during purification and a crystallization protocol very similar to the one reported by us (*7, 9*). The high affinity binding of the aminocarboxylate chelator EDTA to the Ni-binding site of NikA suggested to us that a chemically similar, natural metallophore could be involved in periplasmic Ni transport. Initially, this proposition seemed to be at odds with EXAFS[1]

[†] The CEA and CNRS are thanked for institutional funding. C.B. was supported by a postdoctoral grant from the Agence Nationale de la Recherche, France, and M.C. by a fellowship from the CEA.

[‡] Coordinates and structure factors have been deposited with PDB codes 3dp8 and 3e3k.

* To whom correspondence should be addressed. Phone: 33 4 38785920. Fax: 33 4 38785122. E-mail: juan.fontecilla@ibs.fr.

[§] Laboratoire de Cristallographie et de Cristallogenèse des Protéines.

[||] Present address: Michael G. Rossmann's Laboratory, Departement of Biological Sciences, Lilly Hall of Life Sciences, Purdue University, 915 W. State Street, West Lafayette, IN 47907-2054.

[⊥] Laboratoire de Spectrométrie de Masse des Protéines.

[#] Present address: Laboratoire des Interactions Protéine Métal Institut de Biologie Environnementale et de Biotechnologie, CEA, CNRS, Université Aix-Marseille IICEA Cadarache, Bât 185, 13108 Saint Paul-lez-Durance Cedex, France.

[1] Abbreviations: BTC, butane-1,2,4-tricarboxylate; ABC, ATP-binding cassette; EXAFS, extended X-ray absorption fine structure; ESRF, European Synchrotron Radiation Facility; CA-NikA, cytoplasmic NikA; CE-NikA, chloroform-extracted NikA; NiMP: nickel metallophore; BSA, bovine serum albumin; MS, mass spectrometry.

10.1021/bi801051y CCC: $40.75
Published on Web 08/30/2008

results that indicated Ni binding to recombinant apo NikA (*10*). However, in a recent report, Addy et al. have explained this apparent contradiction (*11*): using X-ray crystallography and other techniques these authors have identified a second NikA Ni-binding site, far from the supposedly physiological one that we found can bind FeEDTA. It has also been reported that NikA binds heme, and a physiological role in the transport of this molecule has been postulated (*12*).

Here, we report the 2.5 Å resolution crystal structure of periplasmic NikA extracted using an EDTA-free protocol (*13*). An electron density omit map indicates that, under these conditions, NikA binds Ni and other metal ions chelated by a small organic molecule of unknown origin and structure. Based on the shape and size of the electron density and by comparison with FeEDTA binding to NikA we postulate that the small chelator is either butane-1,2,4-tricarboxylate (BTC) or, less likely, propane-1,2,3-tricarboxylate (tricarballylate). Indeed, a mass spectrometric (MS) analysis favors BTC as the endogenous metal chelator. In addition, the conformationally very similar crystal structure of *N*-[(carboxylatomethyl)aspartate(3^-)]−(ethylenediamine)cobalt(III) trihydrate (*14*) also lends support to our proposition that the NikA-bound putative endogenous chelator has three metal-bound carboxylate groups. We also have found that commercial racemic BTC binds apo NikA at the same chelator site but without metal, even in the presence of excess Ni.

Based on the results reported here, we postulate that the novel protein−chelator complex we observe in chloroform-extracted NikA crystals may correspond to a natural NikA−Ni−metallophore species.

EXPERIMENTAL PROCEDURES

Periplasmic NikA Expression and Purification. Periplasmic NikA was overproduced by growing 5 L of BL21(DE3) carrying the IPTG-inducible expression vector pET22b-*nikA* (a kind gift from Dr. Long-Fei Wu) in rich LB medium at 37 °C. The periplasmic NikA was extracted by stirring the cells in a solution containing 2.5 mL of chloroform per gram of cells (wet weight) and complete antiprotease cocktail (Roche) at 37 °C for 3 h (*13*). The extraction was stopped by adding 10 volumes of 40 mM Tris, pH 7.4 (buffer A)/volume of chloroform, the cell debris was spun down at 15,000 rpm for 45 min at 4 °C and the supernatant solution was adjusted to 40% (w/v) ammonium sulfate. The resulting soluble fraction was concentrated by precipitation with 80% (w/v) ammonium sulfate and resolubilization in buffer A. The solution was then dialyzed and further purified by two-step anion-exchange chromatography using Q-Sepharose and Resource Q columns, equilibrated with buffer A. NikA was eluted with an ascending sodium chloride gradient. A total of approximately 5 mg of pure NikA per L of culture was obtained by this procedure. The protein was concentrated to 8.0 mg/mL in buffer A.

Cytoplasmic Apo NikA Expression and Purification. Cytoplasmic NikA (CA-NikA) was overproduced in *E. coli* BL21(DE3) strain using the IPTG-inducible vector pET28b (a kind gift from Dr. Jeremy Tame) in LB medium at 37 °C. Cells were resuspended with buffer A containing a protease inhibitor complex (Roche) and passed twice through a French press. Cell debris was removed by centrifugation, and the NikA-containing soluble extract was treated as described above. A total of approximately 75 mg of pure NikA per liter of culture was obtained.

Protein Concentration Determination. NikA concentration was determined by either OD measurements at 280 nm using an $\varepsilon = 72.83\ mM^{-1}\ cm^{-1}$ (*15*) or by using a standard curve obtained from BSA solutions titrated with rose bengal.

Crystallization. Hexagonal prisms of chloroform-extracted NikA (CE-NikA) were obtained using the conditions initially described in Charon et al. (*9*). The best crystals were obtained when 1 μL from the reservoir solution, containing 1.5 M ammonium sulfate in 100 mM sodium acetate, pH 4.7, was mixed with 4 μL of an 8.0 mg/mL CE-NikA solution and the resulting hanging drop was equilibrated against 1 mL of the reservoir solution at 20 °C. In the case of the NikA/Ni/BTC experiment the crystallization conditions were similar to the ones described above except that (1) the 8.0 mg/mL CA-NikA solution was preincubated with 5 molar equiv of BTC and 2.5 molar equiv of $NiCl_2$ (relative to the protein concentration) and (2) three molar equiv of BTC and 1.5 molar equiv of $NiCl_2$ were added to the reservoir solution before mixing it with the protein solution while setting the hanging drops.

X-ray Fluorescence Measurements. The X-ray fluorescence from periplasmic CE-NikA crystals was monitored with a solid state Röntec XFlash detector operating at the BM30A beam line (Figure 1). The detector was placed at 90° from the incident X-ray beam to minimize scattering. The device server to run the detector on ESRF beam lines and the Graphical User Interface to monitor the X-ray fluorescence have been developed by A. Beteva (ESRF) and J. Joly (BM30A), respectively.

Mass Spectrometry. Noncovalent MS measurements of CE-NikA were performed using a Q-TOF Micro mass spectrometer (Micromass, Manchester, U.K.) equipped with an electrospray ion source. It operated with a needle voltage of 3.0 kV, sample cone and extraction cone voltages of 150 and 2 V, respectively. (Backing Pirani pressure was set at 6.48 mbar.) The mass spectra were recorded in the 2700−6000 mass-to-charge (*m*/*z*) range. Sample concentration was 27 μM in 20 mM ammonium acetate and continuously infused at a flow rate of 7 μL/min. Data were acquired in the positive mode, and calibration was performed using a solution of 0.5 mg/mL CsI in water/isopropyl alcohol (1/1 v/v). Mass spectra were acquired and data were processed with MassLynx 4.0 (Micromass) (Figure 2).

Data Collection and Structure Solution. A native data set, here called λ_4 ($\lambda = 0.9330$ Å), was collected from a hexagonal CE-NikA crystal to 2.5 Å resolution at the ID14-EH2 beam line of the European Synchrotron Radiation Facility (ESRF) (Table 1). The structure was solved by the molecular replacement method using the atomic coordinates of the NikA−FeEDTA$(H_2O)^-$ complex previously reported by us (PDB code 1zlq) and the program PHASER (*16*). A well-contrasted solution was obtained with three NikA molecules per asymmetric unit (not shown).

In order to identify the nature of the metal bound to CE-NikA, three additional sets were subsequently collected from a single crystal at the following X-ray wavelengths: $\lambda_1 = 1.7450$ Å and $\lambda_2 = 1.7392$ Å (low- and high-energy sides of the iron absorption edge, respectively) and $\lambda_3 = 1.4852$ Å (maximum f'' for nickel) at the ESRF French BM30A beam line (Tables S1 and S2a in the Supporting Information).

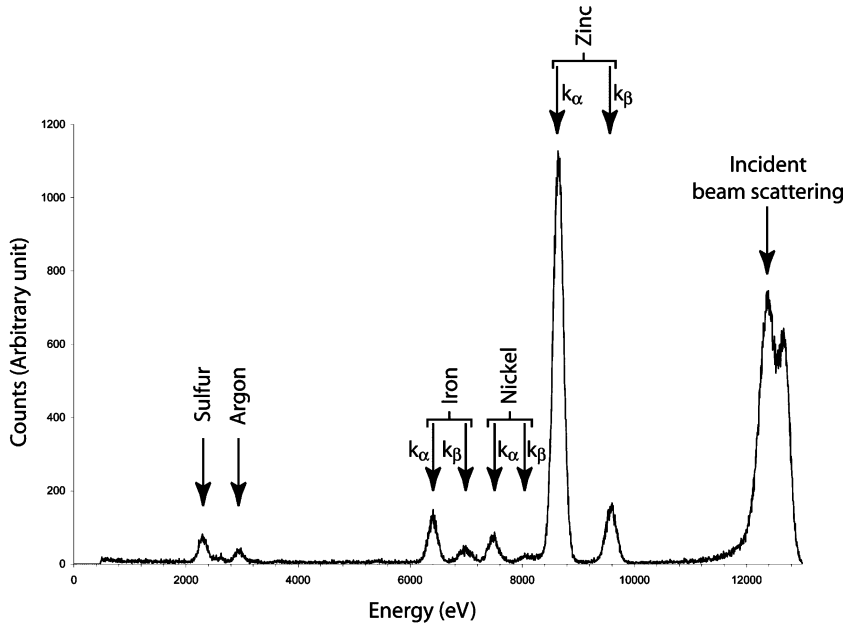

FIGURE 1: X-ray fluorescence spectrum measured on a single hexagonal NikA crystal at beam line BM30A of the ESRF. Note the detection of nickel, iron and zinc. We confirmed the presence of these ions in the crystal structure in X-ray anomalous difference electron density maps (see Supporting Information).

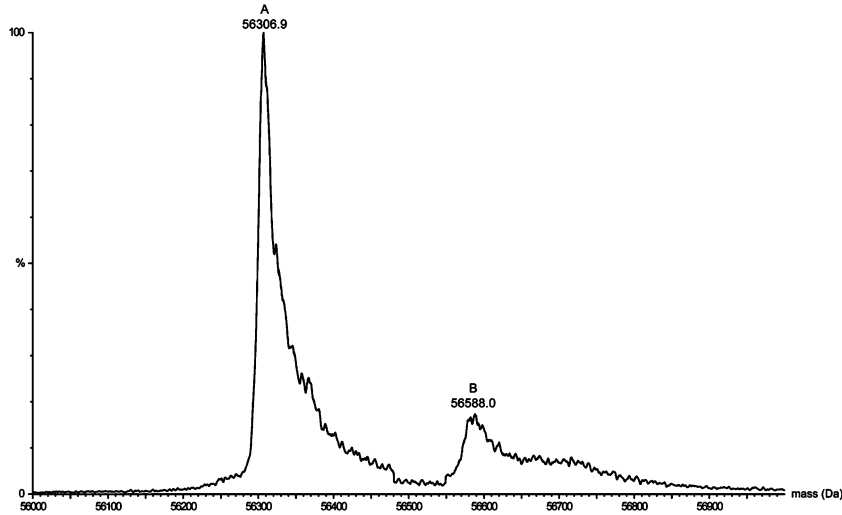

FIGURE 2: Noncovalent mass spectrum of as-prepared CE-NikA. Peak A corresponds to the metal-free protein whereas peak B matches a Ni−butane-1,2,4-carboxylate-Cl^-−NikA complex within experimental error.

Additional X-ray diffraction data collected from a crystal grown in the presence of excess Ni showed significant substitution of Fe and Zn by that ion (Table S2b in the Supporting Information).

A 2.8 Å resolution data set was collected at the ID14-EH3 beam line of the ESRF from a CA-NikA crystal grown in the presence of BTC (Chem Service, West Chester, England) and $NiCl_2$. The structure of the resulting complex was solved as described above for the CE-NikA crystals. All the data sets were collected at 100 K using crystals soaked in the crystallization solution with 25% (v/v) glycerol added as a cryoprotectant.

Crystallographic Refinement. CE-NikA Crystals. The three CE-NikA molecules in the asymmetric unit were refined with REFMAC (*17*) and programs from the CCP4 suite (*18*) without applying noncrystallographic symmetry (the three molecules display different conformations, see below). The model was periodically examined using computer graphics and the program Coot (*19*). Solvent was progressively added using ARP/WARP (*20*) (Table 1). *CA-NikA Crystals.* An equivalent procedure was used for the refinement of the structure from CA-NikA crystals soaked with BTC and $NiCl_2$ (Table S3 in the Supporting Information).

RESULTS

Crystal Structure of CE-NikA. In order to determine the structure of NikA without the tightly bound FeEDTA complex, we extracted the overexpressed protein from *E. coli* periplasm using chloroform (*13*). This allowed us to reproduce the hexagonal crystals obtained several years ago (*9*), before we switched to an EDTA-based periplasmic extraction. Surprisingly, the refined 2.5 Å resolution structures of the three independent molecules from these hexagonal crystals have conformations that are less open than the ones observed for the apo protein (*8*) and the $FeEDTA(H_2O)^-$−NikA complex (*7*) (Figure 3). Furthermore, the three molecules in the asymmetric units are not equiva-

Table 1: Data Collection and Refinement Statistics for the CE-NikA Structure[a]

wavelength (Å)	0.9330
space group	$P6_2$
unit cell (Å)	$a = b = 158.6$; $c = 134.9$
resolution range (Å)	20.0−2.5 (2.6−2.5)
R_{merge}[b] (%)	4.6 (27.8)
R_{meas}[c] (%)	5.3 (32.6)
I/σ	18.6 (5.4)
completeness (%)	97.0 (92.7)
redundancy	3.7 (3.7)
$N_{measured}$	474 337 (50 477)
N_{unique}	127 391 (13 530)
R factor/R_{free} factor (%)	19.9/27.0
no. of protein atoms	12 094
no. of water molecules	265
average B-factor (Å^2):	
all atoms	51.0
protein atoms	51.3
solvent atoms	48.8
ligand atoms (BTC + Ni)	58.9
rms deviations	
bonds (Å)	0.019
angles (deg)	1.963
Ramachandran plot:	
residues in most favorable regions (%)	87.9
residues in additional allowed regions (%)	10.9
residues in generously allowed regions (%)	1.0
residues in disallowed regions (%)	0.2

[a] Last resolution shell shown in parentheses. [b] $R_{sym} = R_{merge} = \sum_h |\hat{I}_h - I_{h,i}|/\sum_h \sum i^{nh} I_{h,i}$. [c] $R_{meas} = \sum_h \sqrt{[n_h/(n_h - 1)]} \sum i^{nh} |\hat{I}_h - I_{h,i}|/\sum_h \sum i^{nh} I_{h,i}$ with $\hat{I}_h = (1/n_h) \sum i^{nh} I_{h,i}$.

lent: due to less tight packing, molecule C has a $B_{average} = 60$ Å^2 compared to values of 48.5 Å^2 and 46.8 Å^2 for molecules A and B, respectively (see Supporting Information).

Metal Content. X-ray fluorescence indicated the presence of Ni, Fe and Zn in the original CE-NikA crystals (Figure 1). Consequently, we calculated three anomalous scattering difference Fourier maps with X-ray diffraction data collected at four different wavelengths (see Experimental Procedures). The maps had ($\lambda_2-\lambda_1$), ($\lambda_3-\lambda_2$) and ($\lambda_4-\lambda_3$) coefficients to determine the presence of Fe, Ni and Zn, respectively. These results are summarized in Table S2a in the Supporting Information. Molecules A and B seem to contain mixtures of Fe, Ni and Zn at the metal-binding site whereas molecule C lacks Fe. A subsequent experiment where X-ray data were collected from a CE-NikA crystal grown in a drop containing a saturating concentration of $NiCl_2$ indicated that Ni significantly displaced Fe and completely substituted Zn at the NikA metal-binding site (Table S2b in the Supporting Information).

Electron Density Corresponding to a Novel Chelator and Geometry at the Ni-Binding Site in CE-NikA. Only molecule B will be discussed here because it is the most ordered one (Table S4 in the Supporting Information) and provided the clearest omit map. The electron density surrounding the metal ion in this map seems to correspond to a small organic molecule. (Corresponding maps for molecules A and C are depicted in Figure S1 in the Supporting Information). As we previously proceeded with the FeEDTA-NikA complex (*7*), we attempted the interpretation of the electron density by a stepwise approach. The presence of at least two carboxylates was suggested by the omit electron density map shape near Arg97 and Arg137 which bind the FeEDTA complex (*7*) (Figures 4 and 5). Furthermore, the remaining electron density was compatible with a third carboxylate also positioned as in the Fe EDTA−NikA complex. The cation−π interaction with Trp398 we noticed in the FeEDTA−NikA complex (*7*) is also present in the CE-NikA structure, with an indol-to-metal distance of 5.5 Å and a θ_0 angle of 16° which fall within expected values (*21*). The absence of a fourth carboxylate moiety in NiMP allows His416 to form a direct bond to the metal ion. The interaction with a histidine side chain is the only direct metal−NikA contact observed so far. The three carboxylates and histidine ligand form a square planar coordination around the metal ion (Figure 5). A similar coordination of a nickel ion is observed in the *E. coli* repressor NikR, involving three histidine and one cysteine ligand (*22*). The His416 approach to the Ni ion results from the relative movement of the "lower" lobe of the protein toward the "upper" lobe forming the least open structure yet described (Figure 3). His416 is respectively 8.5 Å and 5.6 Å closer to the metal binding site in the CE-NikA and Fe-EDTA−NikA complexes than in the apo-structure (Figure S2 in the Supporting Information). The interactions around the metal ion in CE-NikA are summarized in Figure 6.

The best fit to the omit electron density map for the putative Ni metallophore (NiMP) was obtained with the chiral R-BTC (Figure 5) followed by tricarballylate (Fluka) (not shown). Indirect evidence that the NiMP in CE-NikA could be BTC or a closely related molecule was obtained from mass spectrometry. Peak A in Figure 2 corresponds to apo NikA with 56,306.9 ± 6.8 g/mol whereas peak B represents a mass of 56,588.0 ± 5.6 g/mol. The difference between apo-NikA and the species that gives rise to peak B is 280.1 g/mol. If we assume a mass of 58 Da for the Ni ion and of 187 Da for BTC, there is an excess of 35.1 Da that needs to be accounted for. The most likely candidate to explain this difference is Cl^-, with an average mass of 35.5 Da. Indeed, by lowering the contour level from 3.0 to 1.0 σ in the omit electron density map, it is possible to observe the hint of a fifth ligand which would make the Ni coordination square pyramidal (Figure S3 in the Supporting Information).

Formation of a BTC−NikA Complex Using Apoprotein and Racemic Butane-1,2,4-tricarboxylate. A mass spectrometric experiment indicated that the cytoplasmic overexpressed, EDTA-free NikA is mostly in the apo form with a small fraction of acetate−protein complex (Δ mass = 70 Da) but no indication of a NikA-NiMP complex (not shown). Attempts to crystallize this material in our laboratory have been unsuccessful. On the other hand, we obtained hexagonal crystals when a CA-NikA solution was preincubated with commercial racemic BTC and $NiCl_2$ (see Experimental Procedures). Unfortunately, the structure derived from these crystals shows only metal-free BTC bound at the site occupied by FeEDTA in our previous structure (Figure S4 in the Supporting Information). Similar results were obtained with tricarballylate (not shown). This means either that the putative NiMP is not one of these two molecules or that under our experimental conditions the formation of their Ni-containing complexes with NikA is not possible. In spite of the limited 2.8 Å resolution, the shape of the electron density suggested that both BTC enantiomers bind to NikA. Consequently, the *S*- and *R*-racemates of this small molecule were modeled into the omit map (Figure S4 in the Supporting Information). The BTC carboxylate in position 1 occupies a

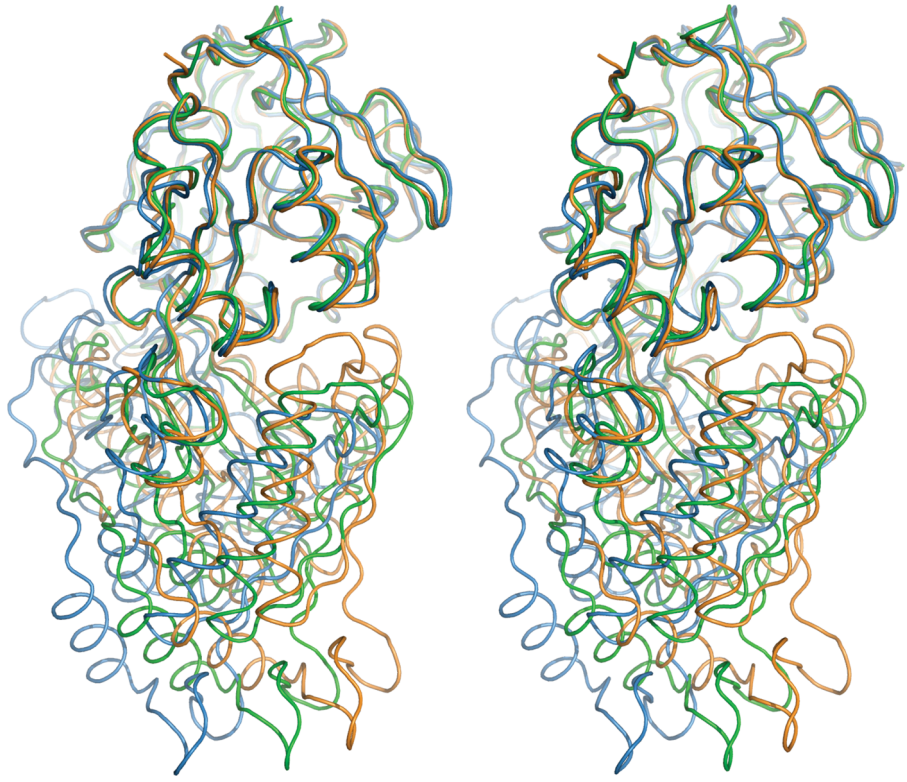

FIGURE 3: Stereopair of the superposition of apo (blue) (*8*), Fe-EDTA-containing (green) (*7*) and chloroform-extracted (CE) NikA (red). The PDB codes are 1uiv, 1zlq and 3dp8, respectively. The polypeptide chains are depicted as tubes. The angle formed between the two protein lobes is of 26°, 18° and 11° for the apo, Fe-EDTA and CE-NikA, respectively. The corresponding number of hydrogen bonds between the lobes is 10, 14 and 21. Figures 3, 4 and 5 were prepared with PyMol (*28*).

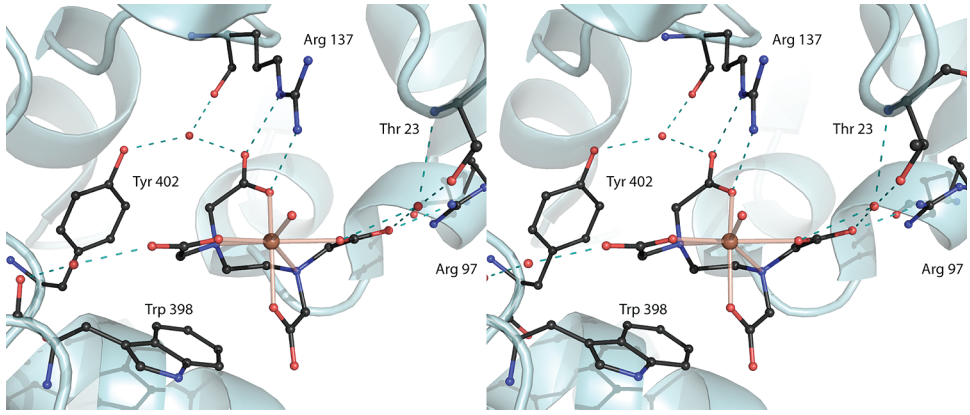

FIGURE 4: Stereopair depicting the FeEDTA$(H_2O)^-$−NikA complex (*7*).

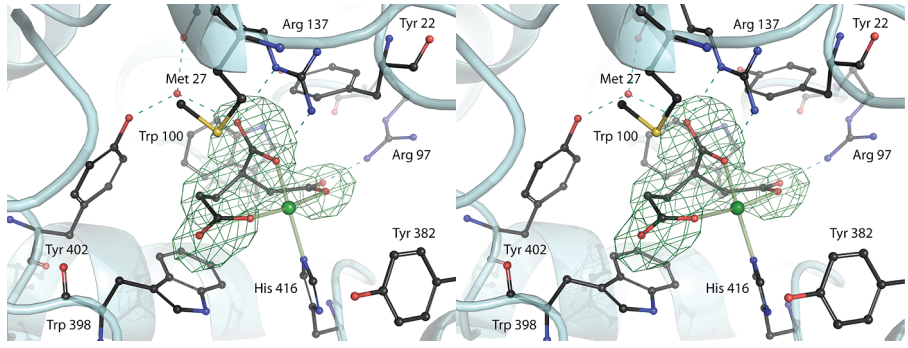

FIGURE 5: CE-NikA Ni-binding site structure with butane-1,2,4-tricarboxylate modeled into the omit electron density map (the nickel ion was included in phases and structure factor calculations). The bonds between nickel (green ball), the three putative carboxylate functions and His416 are depicted as thin lines. The putative Cl^- is not shown (see Figure S3 in the Supporting Information).

region also modeled as a NiMP carboxylate in CE-NikA and the FeEDTA−NikA complex (Figures 4 and 5). As in the former, His416 approaches the Ni−chelator binding site where, however, in the absence of Ni, it forms a hydrogen

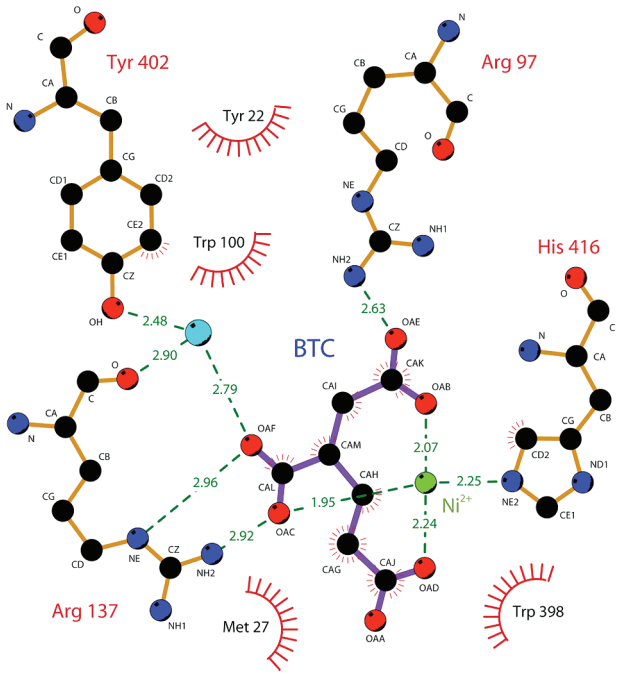

FIGURE 6: LIGPLOT (*29*) drawings depicting the putative BTC−Ni−NikA interactions.

bond with the carboxylate function in position 2 of BTC. Finally, the BTC carboxylate in position 4 seems to have two different conformations depending on the enantiomer. In S-BTC it interacts directly with both Arg137 and Tyr402, whereas in R-BTC, as in the FeEDTA−NikA and CE-NikA−NiMP complexes (Figures 4 and 5), the interaction with Tyr402 is mediated by a water molecule (Figure S4 in the Supporting Information). So, although the conformations of nickel-bound NiMP and added BTC are different, excepting Tyr382, the same NikA residues are involved in the binding in both cases.

DISCUSSION

Taken together, our results clearly indicate that NikA can bind at least two different metal−chelator complexes. When the periplasmic extraction is carried out using EDTA, NikA crystallizes in the $P2_12_12_1$ orthorhombic space group, as a FeEDTA−protein complex (*7*). We have shown that Heddle et al. obtained a similar metal−EDTA crystalline complex when the protein was overexpressed in the cytoplasm and EDTA was added during the purification procedure (*7, 8*). Also, several years ago when we added an excess of EDTA to the CE-NikA crystallization solution, we obtained orthorhombic crystals that we can conclude now contained a metal−EDTA complex. Thus regardless of whether EDTA is added initially for the periplasmic extraction or later during either purification or crystallization, it binds to NikA as metal−EDTA$(H_2O)^-$ and the protein yields orthorhombic crystals of this complex. The hexagonal crystals we reported earlier (*9*) could only be now reproduced from a sample where the periplasmic extraction of NikA was performed using chloroform and in the absence of EDTA. It was surprising to find that under these conditions CE-NikA binds nickel in complex with a putative endogenous NiMP because we expected the hexagonal crystals to correspond to the apoprotein. When CE-NikA-containing drops were equilibrated in the presence of up to a 20-fold molar excess of EDTA, only the hexagonal, NiMP-containing crystals were obtained (even when the solutions were seeded with orthorhombic microcrystals). However, at 50-fold molar EDTA excess, orthorhombic microcrystals used as seeds could be grown, as was the case with NikA extracted in the presence of EDTA. No hexagonal crystals could be obtained under these conditions. This experiment suggests that NiMP can be displaced by a (relatively) high concentration of EDTA.

Our finding that, besides Ni, Fe and Zn bind to the metallophore in NikA is intriguing. This may be due to the fact that the amount of periplasmic NikA produced during its overexpression is larger than the amount of nickel ions available. Excess NikA would then bind the metallophore in complex with either Fe or Zn, which are common ions and will be found as traces in media and buffers. One indication that the metallophore may have a better affinity for nickel than for Fe or Zn is the fact that the former displaced the latter in our crystals.

Attempts to extract and characterize NiMP have been unsuccessful so far. Alkylation of extracts obtained by denaturation of CE-NikA followed by gas chromatography did not produce any species that could be assigned to a derivative of BTC (J. Lorquin, personal communication). MS experiments of denatured CE-NikA were also inconclusive. One of the major problems has been to obtain enough NiMP from the protein samples, as it appears very difficult to dissociate it from NikA. As mentioned above, we know it can be done with a large excess of EDTA but then this chelator will severely interfere with subsequent characterization experiments.

Biological tricarboxylates such as citrate, isocitrate and aconitate appeared as obvious candidates to be the NiMP. However, they do not fit well in the electron density because (1) the endogenous molecule seems to be slightly longer (also a problem for tricarballylate), (2) the OH group of citrate and isocitrate does not have matching density, and (3) the double bond in aconitate makes this molecule incompatible with the observed omit map electron density shape. BTC displays the best fit to the omit map. Although in *E. coli* there is no described metabolic pathway for the synthesis of BTC, a puzzling observation by White et al. (*23, 24*) may be relevant to this problem: *E. coli* cell extracts overexpressing the product of the MJ0503 gene from *Methanococcus jamaschii* synthesized *trans*-homoaconitate and *R*-homocitrate when supplied with 2-ketoglutarate and acetyl-CoA. This was a surprising result because these molecules had not been previously described as metabolites. The authors concluded that native *E. coli* aconitase-like enzymes catalyzed the synthesis of these molecules (*23*). *trans*-Homoaconitate could then be reduced to BTC by a fumarate reductase-like enzyme. Evidence for the biosynthesis and utilization of the (less well-suited) tricarballylate by microorganisms has been found in the digestive tract of ruminants (*25, 26*). Tricarballylate can complex magnesium ions, which are then excreted with pathological consequences for the animal. Although *E. coli* does not normally synthesize tricarballylate (*26*), it could import it (or a precursor) from the medium.

In summary, we have shown that in the hexagonal crystals NikA can bind an unidentified chelator most likely containing three carboxylate functions that may come from the culture medium or it is endogenous to *E. coli*. Indeed we have found

that the structure of *N*-[(carboxylatomethyl)aspartate-(3−)]−(ethylenediamine)cobalt(III) trihydrate (*14*) bears significant similarities with our model of BTC in the CE-NikA structure (Figure S5 in the Supporting Information). Determination of nature and origin of NiMP will have to wait for further investigations. In an effort to better understand the possible physiological relevance of a nickel metallophore we have started a site-directed mutagenesis program of residues involved in Ni and NiMP binding, including His416.

One may wonder why nickel transport should require a metallophore. NikA belongs to a family of periplasmic transporters that bind peptides and other organic molecules (*4, 27*). Maybe evolution could not modify the binding site of such transporters to coordinate a naked metal ion but it was possible to adapt the site to bind a small organic chelator−metal complex.

ACKNOWLEDGMENT

We thank the local contacts of the ESRF beam lines ID14-EH2, ID14-EH3, ID-29 and BM-30A for help with X-ray data collection. We also thank Drs. Jeremy Tame and Long-Fei Wu for the gift of plasmids and Drs. J. Loquin and S. Ménage for their efforts with the gas chromatographic and mass spectrometric experiments on the small organic molecule.

SUPPORTING INFORMATION AVAILABLE

Four tables with crystallographic statistics, and five figures depicting (1) the omit maps for molecules A and C, (2) the position of His416 in apo, FeEDTA and CE-NikA, (3) the final omit map with a small peak corresponding to the putative Cl^-, (4) the binding of added BTC to NikA and (5) a comparison of the structures of NiMP in CE-NikA and *N*-[(carboxylatomethyl)aspartate(3−)]−(ethylenediamine)cobalt(III) trihydrate. This material is available free of charge via the Internet at http://pubs.acs.org.

REFERENCES

1. Eitinger, T., and Mandrand-Berthelot, M. A. (2000) Nickel transport systems in microorganisms. *Arch. Microbiol. 173*, 1–9.
2. Watt, R. K., and Ludden, P. W. (1999) Nickel-binding proteins. *Cell. Mol. Life Sci. 56*, 604–625.
3. Yohannes, E., Barnhart, D. M., and Slonczewski, J. L. (2004) pH-dependent catabolic protein expression during anaerobic growth of *Escherichia coli* K-12. *J. Bacteriol. 186*, 192–199.
4. Wu, L. F., Navarro, C., and Mandrand-Berthelot, M. A. (1991) The hydC region contains a multi-cistronic operon (nik) involved in nickel transport in *Escherichia coli*. *Gene 107*, 37–42.
5. De Pina, K., Desjardin, V., Mandrand-Berthelot, M. A., Giordano, G., and Wu, L. F. (1999) Isolation and characterization of the nikR gene encoding a nickel-responsive regulator in *Escherichia coli*. *J. Bacteriol. 181*, 670–674.
6. Dosanjh, N. S., and Michel, S. L. (2006) Microbial nickel metalloregulation: NikRs for nickel ions. *Curr. Opin. Chem. Biol. 10*, 123–130.
7. Cherrier, M. V., Martin, L., Cavazza, C., Jacquamet, L., Lemaire, D., Gaillard, J., and Fontecilla-Camps, J. C. (2005) Crystallographic and spectroscopic evidence for high affinity binding of FeEDTA(H2O)- to the periplasmic nickel transporter NikA. *J. Am. Chem. Soc. 127*, 10075–10082.
8. Heddle, J., Scott, D. J., Unzai, S., Park, S. Y., and Tame, J. R. (2003) Crystal structures of the liganded and unliganded nickel-binding protein NikA from *Escherichia coli*. *J. Biol. Chem. 278*, 50322–50329.
9. Charon, M. H., Wu, L. F., Piras, C., de Pina, K., Mandrand-Berthelot, M. A., and Fontecilla-Camps, J. C. (1994) Crystallization and preliminary X-ray diffraction study of the nickel-binding protein NikA of *Escherichia coli*. *J. Mol. Biol. 243*, 353–355.
10. Allan, C. B., Wu, L.-F., Gu, Z., Choudhury, S. B., Al-Mjeni, F., Sharma, M. L., Mandrand-Berthelot, M.-A., and Maroney, M. J. (1998) An X-ray absorption spectroscopic investigation of the nickel site in *Escherichia coli* NikA protein. *Inorg chem 37*, 5952–5955.
11. Addy, C., Ohara, M., Kawai, F., Kidera, A., Ikeguchi, M., Fuchigami, S., Osawa, M., Shimada, I., Park, S. Y., Tame, J. R., and Heddle, J. G. (2007) Nickel binding to NikA: an additional binding site reconciles spectroscopy, calorimetry and crystallography. *Acta Crystallogr., Sect. D: Biol. Crystallogr. 63*, 221–229.
12. Shepherd, M., Heath, M. D., and Poole, R. K. (2007) NikA binds heme: a new role for an *Escherichia coli* periplasmic nickel-binding protein. *Biochemistry 46*, 5030–5037.
13. Ames, G. F., Prody, C., and Kustu, S. (1984) Simple, rapid, and quantitative release of periplasmic proteins by chloroform. *J. Bacteriol. 160*, 1181–1183.
14. Maderova, J., Marek, J., and Pavelcik, F. (2003) N-(Carboxylatomethyl)aspartato(3-)-(ehtylenediamine)cobalt(III) tri-hydrate. *Acta Crystallogr. C 59*, 178–180.
15. de Pina, K., Navarro, C., McWalter, L., Boxer, D. H., Price, N. C., Kelly, S. M., Mandrand-Berthelot, M. A., and Wu, L. F. (1995) Purification and characterization of the periplasmic nickel-binding protein NikA of Escherichia coli K12. *Eur. J. Biochem. 227*, 857–865.
16. Storoni, L. C., McCoy, A. J., and Read, R. J. (2004) Likelihood-enhanced fast rotation functions. *Acta Crystallogr. D 60*, 432–438.
17. Murshudov, G. N., Vagin, A. A., and Dodson, E. J. (1997) Refinement of macromolecular structures by the maximum-likelihood method. *Acta Crystallogr. D 53*, 240–255.
18. CCP4, C. C. P. N. (1994) The CCP4 suite: Programs for Protein Crystallography. *Acta Crystallogr. D 50*, 760–763.
19. Emsley, P., and Cowtan, K. (2004) Coot: model-building tools for molecular graphics. *Acta Crystallogr. D 60*, 2126–2132.
20. Zwart, P. H., Langer, G. G., and Lamzin, V. S. (2004) Modelling bound ligands in protein structures. *Acta Crystallogr. D 60*, 2230–2239.
21. Zaric, S. D., Popovic, D. M., and Knapp, E.-W. (2000) Metal ligand aromatic cation-pi interactions in metalloproteins: ligands coordinated to metal interact with aromatic residues. *Chem. Eur. J. 6*, 3935–3942.
22. Schreiter, E. R., Wang, S. C., Zamble, D. B., and Drennan, C. L. (2006) NikR-operator complex structure and the mechanism of repressor activation by metal ions. *Proc. Natl. Acad. Sci. U.S.A 103*, 13676–13681.
23. Graham, D. E., and White, R. H. (2002) Elucidation of methanogenic coenzyme biosyntheses: from spectroscopy to genomics. *Nat. Prod. Rep. 19*, 133–147.
24. Howell, D. M., Harich, K., Xu, H., and White, R. H. (1998) Alpha-keto acid chain elongation reactions involved in the biosynthesis of coenzyme B (7-mercaptoheptanoyl threonine phosphate) in methanogenic Archaea. *Biochemistry 37*, 10108–10117.
25. Cook, G. M., Wells, J. E., and Russell, J. B. (1994) Ability of *Acidaminococcus fermentans* to oxidize trans-aconitate and decrease the accumulation of tricarballylate, a toxic end product of ruminal fermentation. *Appl. Environ. Microbiol. 60*, 2533–2537.
26. Lewis, J. A., Horswill, A. R., Schwem, B. E., and Escalante-Semerena, J. C. (2004) The Tricarballylate utilization (tcuRABC) genes of *Salmonella enterica* serovar Typhimurium LT2. *J. Bacteriol. 186*, 1629–1637.
27. Tame, J. R., Murshudov, G. N., Dodson, E. J., Neil, T. K., Dodson, G. G., Higgins, C. F., and Wilkinson, A. J., and. (1994) The structural basis of sequence-independent peptide binding by OppA protein. *Science 264*, 1578–1581.
28. DeLano, W. L. (2002) http://www.pymol.org.
29. Wallace, A. C., Laskowski, R. A., and Thornton, J. M. (1995) LIGPLOT: a program to generate schematic diagrams of protein-ligand interactions. *Protein Eng. 8*, 127–134.

BI801051Y